Available online at www.sciencedirect.com

ScienceDirect

www.elsevier.com/locate/jes

JES JOURNAL OF ENVIRONMENTAL SCIENCES

www.jesc.ac.cn

# Mercury accumulation and dynamics in montane forests along an elevation gradient in Southwest China

*Shufang Zeng*[1], *Xun Wang*[2], *Wei Yuan*[2], *Ji Luo*[3], *Dingyong Wang*[1,*]

[1] *College of Resources and Environment, Southwest University, Chongqing 400715, China*
[2] *State Key Laboratory of Environmental Geochemistry, Institute of Geochemistry, Chinese Academy of Sciences, Guiyang 550081, China*
[3] *Key Laboratory of Mountain Surface Processes and Ecological Regulation, Institute of Mountain Hazards and Environment, Chinese Academy of Sciences & Ministry of Water Conservancy, Chengdu 610041, China*

ARTICLE INFO

*Article history:*
Received 11 July 2021
Revised 6 October 2021
Accepted 11 October 2021
Available online 22 February 2022

*Keywords:*
Mercury deposition
Montane forest
Mercury accumulation
Climate impact

ABSTRACT

Understanding atmospheric mercury (Hg) accumulation in remote montane forests is critical to assess the Hg ecological risk to wildlife and human health. To quantify impacts of vegetation, climatic and topographic factors on Hg accumulation in montane forests, we assessed the Hg distribution and stoichiometric relations among Hg, carbon (C), and nitrogen (N) in four forest types along the elevation of Mt. Gongga. Our results show that Hg concentration in plant tissues follows the descending order of litter > leaf, bark > root > branch > bole wood, indicating the importance of atmospheric Hg uptake by foliage for Hg accumulation in plants. The foliar Hg/C (from 237.0 ± 171.4 to 56.8 ± 27.7 μg/kg) and Hg/N (from 7.5 ± 3.9 to 2.5 ± 1.2 mg/kg) both decrease along the elevation. These elevation gradients are caused by the heterogeneity of vegetation uptake of atmospheric Hg and the variation of atmospheric $Hg^0$ concentrations at different altitudes. Organic soil Hg accumulation is controlled by forest types, topographic and climatic factors, with the highest concentration in the mixed forest (244.9 ± 55.7 μg/kg) and the lowest value in the alpine forest (151.9 ± 44.5 μg/kg). Further analysis suggests that soil Hg is positively correlated to C ($r^2 = 0.66$) and N ($r^2 = 0.57$), and Hg/C and Hg/N both increase with the soil depth. These stoichiometric relations highlight the combined effects from environmental and climatic factors which mediating legacy Hg accumulation and selective Hg absorption during processes of organic soil mineralization.



## Introduction

Mercury (Hg) is a well-documented pollutant which causes the serious harm to the health of human and ecosystems. The increasing anthropogenic emission during last two centuries has driven the Hg concentration in the atmosphere by approximately 3 to 5 times (AMAP, 2019), and resulted in the elevated deposition of atmospheric Hg in the remote forest ecosystems (Fu et al., 2010a; Gerson et al., 2017). The current dry and wet depositions of atmospheric Hg in forest systems are about 2 to 3 times higher than values before the Industrial Revolution era (AMAP, 2019), thus significantly increasing the risk of Hg

* Corresponding author.
*E-mail:* dywang@swu.edu.cn (D. Wang).

https://doi.org/10.1016/j.jes.2021.10.015
1001-0742/

pollution in remote ecosystems. The Hg accumulated in upland forest soils can be transported to downstream aquatic ecosystems where it can be readily bioaccumulated and biomagnified upon methylation, thus posing a threat to ecological security (Li et al., 2012; Bravo et al., 2017). Therefore, the focus of the Hg accumulation and migration in upland forest is critical to understand the Hg biogeochemical cycling and ecological risks in remote regions.

Due to the complex terrain and climatic influences, previous studies have preliminarily made assessments on the Hg biogeochemical accumulation in upland forests. Several studies highlighted that the lower temperature along the elevation enhanced the rainfall and cloud-water Hg deposition, leading to a shift of the dominant Hg deposition pathway from litterfall Hg deposition in low-elevation hardwood forests to wet Hg deposition in alpine forests (i.e., mountain cold-trapping effect) (Lawson et al., 2003; Blackwell and Driscoll, 2015). However, the Hg isotopic evidences suggested the litterfall Hg deposition as the main source for Hg accumulation in montane forests, and the temperature and rainfall by controlling the litter biomass production to drive the litterfall Hg deposition (Zhang et al., 2013; Wang et al., 2017). These debates indicate that Hg accumulation in the montane forest floor is the result of multiple impacts from environmental factors. The altitude gradient in montane forest leads to distinct vegetation and climatic variations (Blackwell and Driscoll, 2015; Zu et al., 2019), thus playing an important role in shaping vegetation distribution, C and N biogeochemical processes in soils. These processes also affect the fate of legacy Hg in forest floors along the elevation (Garten and Hanson, 2006; Smith-Downey et al., 2010).

The Tibetan Plateau (TP), with an average elevation of more than 4000 meters, is known as the "Third Pole" on the earth. Though the TP is geographically remote and has few human activities, elevated atmospheric pollutants are still observed in the biota of TP since the long-distance transport of pollutants from East, South and Southeast Asia under the influence of the monsoon (Gong et al., 2014). Several studies have reported the enhanced Hg accumulation in mountain forests of the TP (Fu et al., 2010; Wang et al., 2017). However, the Hg accumulation processes and influencing factors are still with a large knowledge gap, specifically, in response to the driving factors for Hg accumulation along the elevation in montane forests. Given the Hg accumulation along the montane gradient as the result of multiple influences from climate, vegetation and topography, we comprehensively assessed the Hg distribution in various vegetation components (including leaves, branches, bark, bole wood, roots, herb leaves, shrub leaves, shrub branches, moss, and litter) and soil profiles in different elevation of montane forests at Mt. Gongga, in the east of the TP. We then analyzed the stoichiometric relationships among Hg, C and N to demonstrate the Hg transport and allocation in different forests. Finally, we comprehensively discussed the potential controlling factors for Hg accumulation along the elevation gradient.

## 1. Materials and methods

### 1.1. Study area

The study region is located at Hailuogou National Forest Park (101°52′44″E, 29°35′44″N) of Mt. Gongga in southwestern China. Mt. Gongga is on the eastern edge of the Qinghai-Tibet Plateau, with the summit of 7556 m above sea level, and as the highest mountain in Sichuan Province (Fig. 1). The climate, vegetation, and soil types at Mt. Gongga significantly shift along the altitude. Mt. Gongga belongs to the subtropical monsoon climate zone, and has distinct rainy (May to October) and dry (November to April) seasons. Given the specific geographical environment and climatic conditions, Mt. Gongga forms a four-dimensional forest belt from the evergreen broadleaf, mixed, coniferous to alpine forests (Table 1). Briefly, the broadleaf forest zone is located at low elevations of 1800 to 2250 m, with an annual precipitation of 1300 to 1500 mm, and the dominant tree species are *Lithocarpus cleistocarpus, Salix matsudana Koidz*, and *Cinnamomum camphora*. The mixed forest zone is located at mid-elevations of 2300 to 2800 m, with an annual precipitation of 1500 to 1900 mm, and is dominated by *Abies fabri, Picea brachytyla, Betula utilis, Lithocarpus cleistocarpus*, and *Acer saccharum Marsh*. The coniferous forest is located at elevations of 2800 to 3600 m, with an annual precipitation of 1720 to 1950 mm, and the dominant tree species are *Picea asperata* and *Abies fabri*. The final alpine forest zone is located at high elevations of 3600 to 3800 m, with an annual precipitation of 700 to 900 mm, and is dominated by *Abies fabri* and *Rhododendron Cephalanthum* (Table 1). The soil types from the evergreen broadleaf to alpine forest

**Table 1 – Description of sampling sites along the elevations at Mt. Gongga. The data of annual temperature and annual precipitation are obtained from Xie et al. (2014).**

| Forest type | Altitude (m) | Soil type | Dominant plants | Annual temperature (°C) | Annual precipitation (mm) |
|---|---|---|---|---|---|
| Evergreen broadleaf | 1800-2250 | Yellow-brown soil | *Lithocarpus cleistocarpus, Salix matsudana Koidz, Cinnamomum camphora* | 8.0-10.5 | 1300-1500 |
| Mixed broadleaf-conifer | 2300-2800 | Brown soil | *Abies fabri, Picea brachytyla, Betula utilis, Lithocarpus cleistocarpus, Acer saccharum Marsh* | 5.0-8.0 | 1500-1900 |
| Evergreen coniferous | 2800-3600 | Dark-brown soil | *Picea asperata, Abies fabri* | 0.5-5.4 | 1720-1950 |
| Alpine | 3600-3800 | Meadow soil | *Abies fabri, Rhododendron Cephalanthum* | -3.2-0.4 | 700-900 |

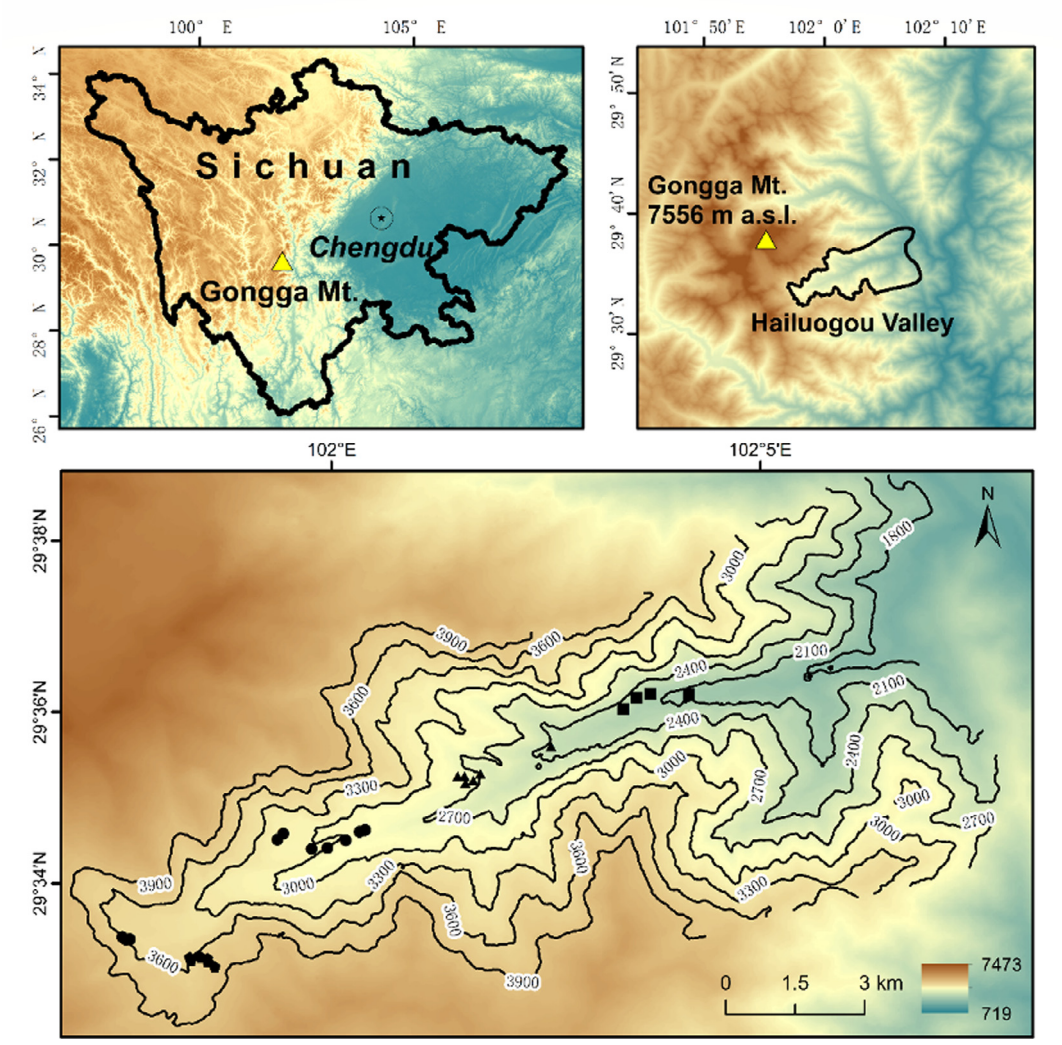


**Fig. 1 – The location of the study area and sampling sites on the eastern slope of the Mt. Gongga. Square symbols represent broadleaf forest sites, and triangles are the mixed forest sites, and circles are the coniferous forest site, and pentagons are the alpine forest sites.**

are yellow-brown soil, brown soil, dark-brown soil, and alpine dark-brown soil, respectively.

### 1.2. *Sample collections*

Our sampling period was from the year of 2014 to 2016. We set 5 to 6 reduplicated 10 m × 10 m sampling plots in four forest zones and located them with GPS, respectively (Fig. 1). In each plot, about 500 g branches, bark, bole wood, and leaves were collected to mix a composite sample, respectively, according to different positions and tree species. Roots were collected in the surface soil (0-30 cm) based on the structure of root order, i.e., small (diameter < 2 mm) and large (diameter > 30 mm) roots. Meanwhile, we set three 1 m × 1 m subplots in each sampling plot to collect the ground moss, shrub and herb samples. Tree mosses were also sampled above 1 to 2 m of the trunk in subplots. Fresh litter (undecomposed) in each sampling plot were collected as an "S" pattern to mix a composite sample of about 500 g. Finally, we selected a relatively flat area to collect the O, A, B, and C layers of soil samples according to the soil occurrence levels. All samples were put into clean plastic bags and stored immediately in a 4 °C portable refrigerator.

### 1.3. *Laboratory analysis*

Samples were transported to the laboratory and then dried in an oven at 40°C to a constant weight (the mass difference between two 8-hour heating < 0.03%). After drying, all samples were completely ground into a fine powder to pass through a 200-mesh sieve. In order to prevent cross-contamination during sample pretreatment, we rinsed the mortar and sieve with pure water after the treatment of each sample, and then carefully wiped them with alcohol. The total Hg concentration was determined by Lumex RA-915$^{+}$ Hg analyzer (Russia, the detection accuracy was 1 μg/kg). The total carbon (TC) and total nitrogen (TN) concentrations were determined by Elementar Vario Macro Cube C analyzer (Germany, the detection limit

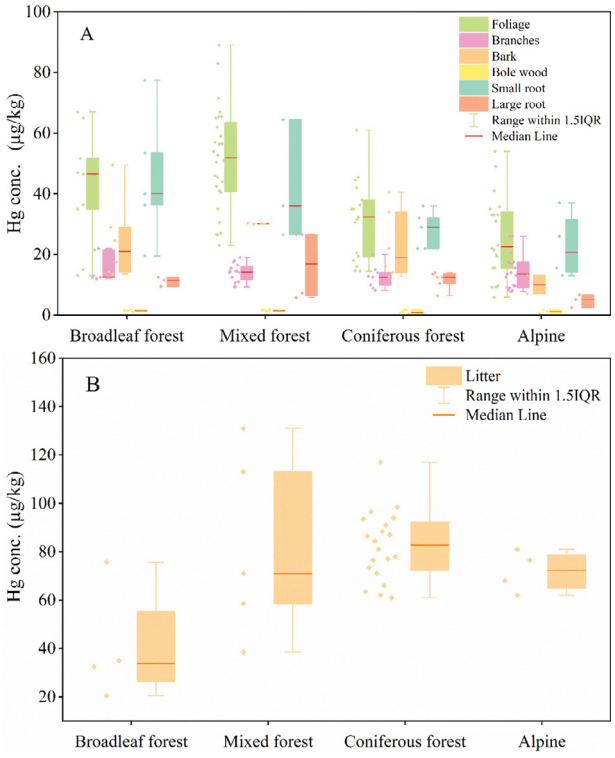


**Fig. 2 – Mercury concentrations in vegetation biomass among different montane forests. The main vegetation components in A: foliage, branches, bark, bole wood, small root and large root; and in B: litter.**

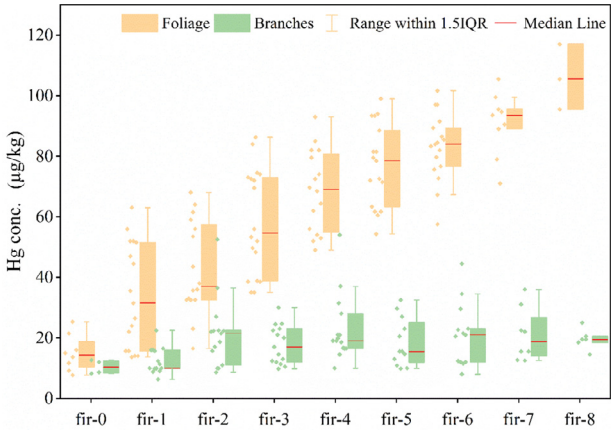


**Fig. 3 – Mercury concentrations of fir foliage and branches for different age stage in evergreen coniferous forest.**

was ≤ 10 μg/g). All samples were measured more than two times until the difference was less than 5%, and the standard reference material was measured after every 10 samples. The standard reference material for soil sample was GBW07405 (GSS-5), and for the vegetation was GBW10020 (GSB-11). For the C and N determination, the standard reference material of soil was IVA99994 and of plant was AR-2026. The recoveries of all standard reference materials ranged from 95% to 105%.

### 1.4. *Statistical analysis*

We used Origin 2019b and EXCEL for the data visualization, and IBM SPSS Statistics 25.0 for the statistical analysis. The significance of all statistical analyses was based on a 95% confidence interval. We used one-way ANOVA and post-hoc Tukey HSD to conduct the statistically difference analysis when data normally distributed, otherwise by Kruskal-Wallis test. In addition, the regression analysis was used to select the potential influencing factors of Hg in forests.

## 2. Results

### 2.1. *Mercury variations in biomass*

As shown in Fig. 2, the average of foliar Hg concentration in four forests is 2 to 66 times higher than values of bole wood and branches ($P < 0.01$, by One-way ANOVA, the same below), but 1 to 3 times lower than the value of litter ($P < 0.01$). Along the elevation gradient, Hg concentrations in foliage significantly vary among the different forest types ($P < 0.01$). The highest value in foliage is found in the mixed (51.2 ± 16.6 μg/kg) and broadleaf forests (41.9 ± 18.1 μg/kg), followed by the coniferous forest (29.3 ± 12.4 μg/kg, with 1-3 years leaf span), and the lowest concentration in the alpine forest (26.3 ± 13.4 μg/kg). Fig. 3 illustrates that the Hg concentration of coniferous foliage linearly increases with the growing age, while an insignificant gradient for coniferous branches. Briefly, the Hg concentration of the 8-year-old coniferous foliage is about 7 times than that in the current year foliage. Given the lifespan, the estimated annual rate of coniferous foliar Hg accumulation rate is 10.6 μg/kg/yr. This rate is much lower than the rate of one-year growth broadleaf (41.9 ± 18.1 μg/kg/year, $P < 0.01$, Fig. 2A, Fig. 3).

For other vegetation components, the highest litter concentrations are found in the mixed (82.4 ± 34.4 μg/kg) and coniferous forests (82.3 ± 13.9 μg/kg), followed by the alpine forest (71.9 ± 7.4 μg/kg), and the lowest concentration in the broadleaf forest (40.9 ± 20.8 μg/kg). The average of Hg concentration of tree moss (226.6 ± 62.9 μg/kg) in four forest sites is 1 to 4 times higher than the value of ground moss (123.1 ± 34.7 μg/kg, $P < 0.01$). For underground tissues, the average of Hg concentration of small root (34.5 ± 16.6 μg/kg) in four forest sites is 2 to 7 times higher than that of large root (11.1 ± 6.6 μg/kg, $P < 0.05$). However, there are no significant differences for Hg concentrations in herb leaves ($P = 0.19$), shrub leaves ($P = 0.21$) and shrub branches ($P = 0.51$) among four forest sites.

### 2.2. *Mercury concentration variations in soils*

Fig. 5 exhibits the distribution of Hg concentrations in soil horizons of four forest sites. For the broadleaf, mixed and coniferous forest, A-horizon (214.5 ± 11.3, 349.1 ± 106.5 and 210.1 ± 9.7 μg/kg, respectively) has the highest soil Hg concentration, followed by O-horizon (175.6 ± 13.3, 244.9 ± 55.7 and 188.0 ± 29.3 μg/kg, respectively), then in B-horizon (67.3 ± 20.8, 117.3 ± 43.2 and 168.5 ± 12.5 μg/kg, respectively), and finally in C-horizon (41.7 ± 21.2, 71.2 ± 38.9 and 61.4 ± 44.6 μg/kg,

respectively). For the alpine forest, soil Hg concentrations decrease with depth (151.9 ± 44.5, 69.6 ± 29.7, 45.8 ± 39.2 and 14.5 ± 7.3 μg/kg for O, A, B and C horizons, respectively). Along the elevation, the mixed forest has the highest Hg concentrations in O and A horizons, followed by the broadleaf and coniferous forests, and the lowest concentrations are in the alpine forest ($P < 0.05$). However, there are no significant differences for Hg concentrations in the B ($P = 0.08$) and C ($P = 0.30$) horizons among each forest type.

### 2.3. *Relationships among Hg, C, and N in biomass and soils*

The Hg/C ratios of foliage decrease among the elevation ($P < 0.05$, Fig. 6), with the highest value in the broadleaf forest (237.0 ± 171.4 μg/kg), followed by the mixed (108.2 ± 35.9 μg/kg) and coniferous forests (85.6 ± 45.4 μg/kg), and the lowest value in the alpine forest (56.8 ± 27.7 μg/kg). The Hg/C value of ground moss also has a decreasing trend with the elevation, but no significant difference for the Hg/N ratio ($P = 0.12$). The average of the Hg/C ratios in O, A, B and C horizons in four forests are 453.9 ± 92.6, 714.3 ± 221.6, 1880.6 ± 313.7 and 1255.2 ± 881.0 μg/kg; for Hg/N ratios are 10.6 ± 3.4, 14.2 ± 3.3, 31.3 ± 5.3 and 25.0 ± 15.3 mg/kg, respectively. In addition, soil Hg/C and Hg/N both increase with the depth of soil profiles. Further analysis suggests the soil Hg concentration shows a significantly positive correlation to both C ($r^2 = 0.66$, $P<0.01$) and N contents ($r^2 = 0.57$, $P < 0.01$, Fig. 7). Specifically, the Hg/C ratios exponentially increase with decreasing C/N ratios in soil profiles ($r^2 = 0.54$, $P < 0.05$, Fig. 8).

## 3. Discussion

### 3.1. *Accumulation of mercury in biomass*

Our Hg concentrations in broadleaf and coniferous foliage are consistent with values reported in similar remote forests globally in Table 2. However, the bole wood Hg concentration at our sites is much lower than that reported in southwestern China (Zhou et al., 2016) and the north-central of USA (Grigal, 2003). The Hg concentration of litter in our coniferous forest is much higher than data found at Mt. Whiteface (Gerson et al., 2017) and Sierra Nevada, USA (Obrist et al., 2009). These differences may be attributed to the remote location of Mt. Gongga where has a lower atmospheric $Hg^0$ concentration (Zhu et al., 2008) and the different tree species induced the discrepancy of Hg uptake and allocation in forests (Bishop et al., 1998).

The $Hg^0$ vapor is converted to $Hg^{2+}$ compounds and fixed in leaf tissues after the foliage uptake via the stomatal and cuticular routes (St Louis et al., 2001; Zhou et al., 2021). Hence, the foliar physiological characteristics, such as stomatal conductance, specific leaf area and leaf life cycle, are the predominant factors to affect the accumulation of Hg in foliage (Laacouri et al., 2013). Similar dominant tree species between the coniferous and alpine forests contribute to their comparable foliar and litter Hg concentrations. By comparing the Hg concentrations between one-year time of broadleaf and coniferous foliage (Fig. 2A, Fig. 3), the higher Hg annual accumulation rate is observed in broadleaf foliage, consistent

**Table 2 – Comparison of Hg concentrations (μg/kg) in above-ground, litter and soil profiles in this study and other forests.**

| Locations | Forest type | Altitude (m) | Bole wood | Foliage | Litter | Bark | Soil | References |
|---|---|---|---|---|---|---|---|---|
| Mt. Gongga, Southwestern China | Evergreen broadleaf | 1800-2250 | 1.5 ± 0.2 | 41.9 ± 18.1 | 40.9 ± 20.8 | 24.7 ± 12.4 | 24.3-230.0 | This study |
| | Mixed broadleaf-conifer | 2300-2800 | 1.3 ± 0.6 | 51.2 ± 16.6 | 82.4 ± 34.4 | 30.2 ± 0.2 | 27-453.7 | |
| | Evergreen coniferous | 2800-3600 | 1.0 ± 0.6 | 29.3 ± 12.4 | 82.3 ± 13.9 | 23.2 ± 10.5 | 5.2-240.5 | |
| | Alpine | 3600-3800 | 1.2 ± 0.4 | 26.3 ± 13.4 | 71.9 ± 7.4 | 10.0 ± 3.0 | 5.4-236 | |
| Mt. Gongga, Southwestern China | Mixed broadleaf-conifer | 2650-3000 | - | 27.6-32.1 | 38.7-39.9 | - | 120-260 | (Fu et al., 2010) |
| | Evergreen coniferous | 3200 | - | 25.0 ± 7.7 | 32.1-39.0 | - | 120-260 | |
| | Alpine | 3580 | - | 23.0 ± 10.2 | 29.0 | - | 120-260 | |
| Mt. Dongling, China | Mixed broadleaf-conifer | 1100 | 2.9 ± 2.5 | 36.6-65.9 | 48.7 ± 9.8 | 2.7-35.6 | 8-104 | (Zhou et al., 2017) |
| Tieshanping, Southwestern China | Mixed broadleaf-conifer | 500 | 8-15 | 78-244 | 115 ± 11 | 27 ± 9 | 58-332 | (Zhou et al., 2016) |
| Mt. Ailao, China | Deciduous broadleaf | 2450-2650 | - | 59-75 | 43-62 | - | 118-279 | (Zhou et al., 2013a) |
| Sierra Nevada, USA | Evergreen coniferous | 1700-2010 | 0.23 ± 0.1 | 11.2-18.9 | 21.6-39.4 | 12.4-21.3 | 8-134 | (Obrist et al., 2009) |
| Mt.White, USA | Mixed broadleaf-conifer | 500 | 1.5-4.6 | 18.0-33.2 | - | - | - | (Yang et al., 2017) |
| Adirondack Mountains, USA | Deciduous broadleaf | 530 | - | 29.1-47.3 | 46.9-61.6 | - | - | (Bushey et al., 2008) |
| Prince Albert National Park, Canada | Evergreen coniferous | 500 | 2 | 10 | - | 16-38 | 120-300 | (Friedli et al., 2007) |
| Mt. Whiteface, USA | Deciduous broadleaf | 400-900 | - | 15-38 | 31 ± 1.4 | - | 156 ± 8 | (Blackwell and |
| | Evergreen coniferous | 1000-1300 | - | 4-34 | 48 ± 3.9 | - | 298 ± 15 | Driscoll, 2015; |
| | Alpine | 1350-1483 | - | - | 67 ± 3.9 | - | 337 ± 16 | Gerson et al., 2017) |

with previous studies (Rea et al., 2002; Bushey et al., 2008; Blackwell and Driscoll, 2015). This is because the stomatal conductance and specific leaf area of broadleaf foliage are typically higher than in conifer needles (Kloeppel et al., 2000; Millhollen et al., 2006; Agnan et al., 2016), thus leading to a larger Hg absorption rate. However, needles have a several-year lifespan, which setting off the lower instantaneous uptake of Hg rate (Obrist et al., 2012). Thus, we observed coniferous litter Hg concentration could be higher than the Hg in broadleaf litter. In addition, earlier measurements have suggested the elevated atmospheric $Hg^0$ concentration at lower altitude of Mt. Gongga due to the local smelting activities and fuel combustion (Fu et al., 2008; Fu et al., 2009). The higher atmospheric $Hg^0$ concentration at lower altitude also can promote the greater Hg concentration in broadleaf foliage (Manceau et al., 2018; Zhou et al., 2021).

The Hg isotopes have identified that Hg in bole wood and branch is mainly derived from the foliage uptake of atmospheric $Hg^0$ and subsequent translocation by the phloem (Wang et al., 2020; Zhou et al., 2021). Hence, the Hg concentrations in aboveground woods are lower than foliage. For other aboveground component, bark also shows a higher concentration than bole wood and branch because of the direct absorption atmospheric $Hg^0$ and particle Hg due to the loose porous structure of bark (Zhou et al., 2016). For underground tissues, small roots have larger specific surface area than large roots, thus leading to much stronger absorptive potential for Hg in soils (Rewald et al., 2011; Wang et al., 2012). A supplemental explanation for the lower Hg concentration in large roots is the higher wood mass dilution since a large proportion of Hg is bound to the cell walls and membranes of fine roots, and few Hg is transported into the large roots (Wang et al., 2012). For higher Hg concentration in moss compares with other vegetation, the main reason is that moss can efficiently take up atmospheric Hg and store in the tissue (Bargagli, 2016) because the simple cell structure makes $Hg^0$ vapor and solution $Hg^{2+}$ easily pass through entire surface of cell walls (Bargagli, 2016; Stankovic et al., 2018; Wang et al., 2019a; Zhou et al., 2021). In addition, the different species and smaller touching area for the ground moss than for the tree moss likely contribute to its lower Hg concentration.

### 3.2. *Accumulation of mercury in soils*

The soil Hg levels at Mt. Gongga are consistent with values reported in other subtropical forests in China, but significantly greater than those reported in some low atmospheric Hg deposition regions of North America (Obrist et al., 2009), such as in Sierra Nevada forests (8-134 μg/kg in organic and mineral layers) in Table 2. Along the elevation, we suggest the soil types do not significantly affect the Hg pattern since no significant differences for Hg concentrations in the B ($P = 0.08$) and C ($P = 0.30$, by One-way ANOVA) horizons among each forest type. Instead, the climate and vegetation shifts along the elevation are the dominant factor to drive Hg accumulation gradients.

The lowest organic soil Hg concentration in the alpine forest is caused by the low litter biomass and harsh climate (low precipitation and temperature, Table 1). The harsh climate significantly constrains the plant litter production

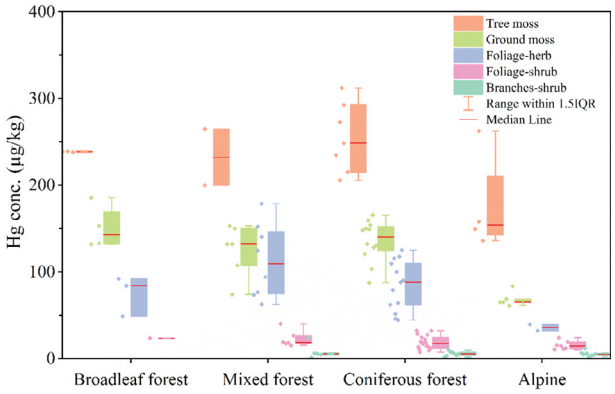


**Fig. 4 – Mercury concentrations in the shrub layer. The main components include tree moss, ground moss, herbaceous foliage, shrub foliage and shrub branches.**

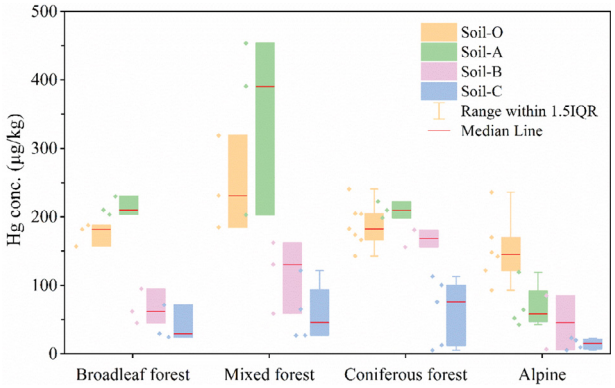


**Fig. 5 – Mercury concentrations in O-horizon soils, A-horizon soils, B-horizon soils and C-horizon soils in different forest zones.**

(Wang et al., 2019b). Isotopic evidence has suggested that litterfall Hg deposition is the dominant source for soil Hg accumulation (Wang et al., 2017; Wang et al., 2019b). Hence, the decrease of the litter biomass leads to a lower litterfall Hg deposition. In addition, the decrease of precipitation in alpine forests can reduce the atmospheric Hg input to forest floor via precipitation and throughfall. Moreover, compared with the other three forests, the sparse vegetation and harsh climate in the alpine forest can lead to a poor soil development and less rock weathering process, thus inducing smaller geogenic Hg into soils (Zheng et al., 2016). However, given the comparable Hg concentration in C horizon, the contribution caused by the rock weathering processes induced geogenic Hg in deep soils would not exhibit large difference along the elevation.

The highest Hg concentration in the organic soil in the mixed forest can be attributed to two possible reasons. One is that the vegetation biomass of Mt. Gongga reaches the maximum in the mixed forest (Zhou et al., 2013b). Therefore, the combined effect of higher biomass production and larger Hg concentration in litter (Fig. 2B) contributes to the elevated atmospheric Hg input to soils. The other is that the mixed forest has a lower rate of Hg re-emission from organic soils.

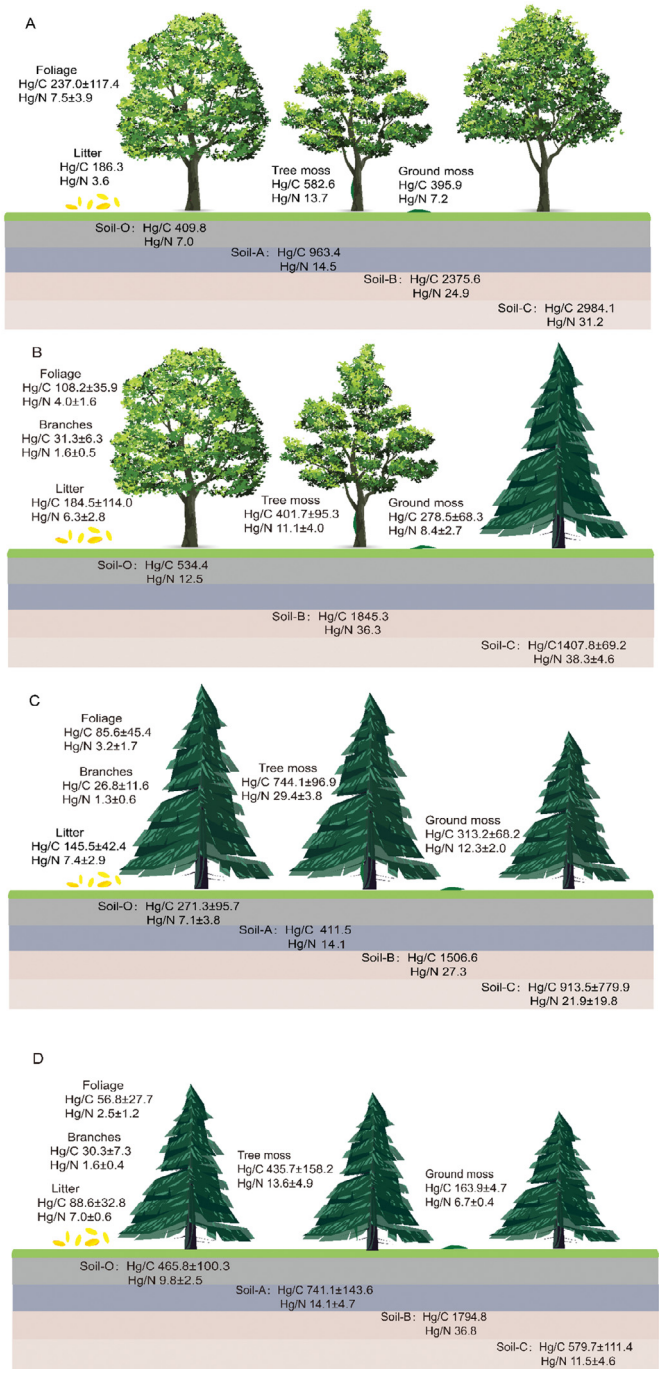


**Fig. 6 – Hg/C ratios (μg/kg) and Hg/N ratios (mg/kg) in aboveground, litter and soils of (A) Evergreen broadleaf mixed forest; (B) Mixed broadleaf-conifer forest; (C) Evergreen coniferous forest; (D) Alpine forest.**

Fu et al. (2010) suggested that the mixed forest had the smaller $Hg^0$ re-emission rate when compared to the broadleaf forest at lower elevation at Mt. Gongga. In addition, the mixed forest has a smaller Hg runoff than the coniferous forest due to the lower precipitation (Table 1).

The soil A horizon shows comparable Hg concentrations to the O horizon in the broadleaf, mixed and coniferous forests ($P > 0.05$), while the much lower values in the A horizon of the alpine forest ($P < 0.01$). This difference can be attributed to the specific source of Hg in the A horizon. The broadleaf, mixed and coniferous forests are as primitive forests and with well-developed soil layers. Therefore, the high Hg concentrations and large soil C contents (21.1%-40.5%) in the A horizon of these forests are mainly derived from the long-term decomposition of organic soils. However, the harsh climate and sparse vegetation in the alpine regions lead to the thin soil layers. Thus, Hg in the A horizon of alpine forests mainly comes from geogenic processes which with much lower Hg concentrations. This is also consistent with the low soil C content in the A layer (5.9%-10.8%).

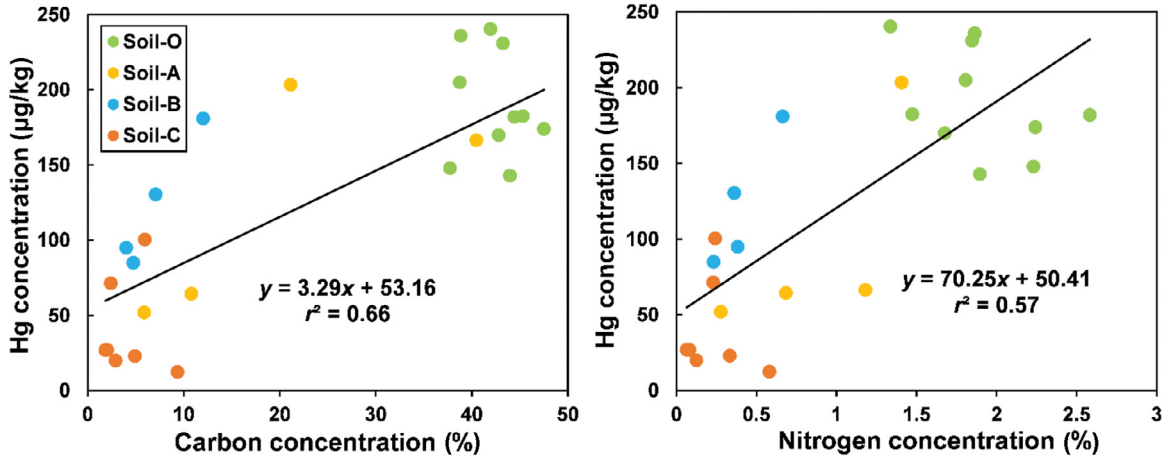


**Fig. 7 – Linear relationship between soil Hg and C or N concentrations in soil layers of O, A, B, and C.**

### 3.3. *Stoichiometry among Hg, C, and N in biomass and soils*

Hg/C and Hg/N ratios can be as a useful tracer to depict Hg accumulation processes in forests since these relation variations indicate the Hg mass flow among the ecosystem compartments (e.g. from leaves to soils) thus to infer the fate of Hg sequestration in forests (Obrist et al., 2012). Foliar and ground moss Hg/C ratios decrease along the elevation in Fig. 6. We suggest such a gradient is relevant to the heterogeneities of vegetation and atmospheric $Hg^0$ in different forests. As discussed above, the higher Hg/C ratio in broadleaf foliage is caused by the combined effects from higher stomatal conductance and specific leaf area of broadleaf foliage and higher atmospheric $Hg^0$ at the low altitude region. Similarly, the species (Pradhan et al., 2017) and atmospheric $Hg^0$ impacts also can explain the altitude gradient of Hg/C ratio in the ground moss.

Given organic matters with a high affinity for Hg, earlier studies have well documented that soil organic matter (SOM) is one of the most critical factors to affect the Hg accumulation in soils (Grigal, 2003; Obrist et al., 2009; Obrist et al., 2011). For instance, the mossy coppice forest of Mt. Ailao shows Hg/C ratios of 500 ± 200 μg/kg in the O-horizon and 900 ± 200 μg/kg in the A-horizon, and the broadleaf forest has the Hg/C ratios of 1300 ± 300 and 2400 ± 300 μg/kg in the O-horizon and A-horizon, respectively (Lu et al., 2016). Navrátil et al. (2014) found much higher Hg/C ratios ranging from 470 to 5500 μg/kg in Oi to C horizons at five Czech sites. These increasing Hg/C ratios with the depth of soil profiles suggest that the older organic matter which is highly decomposed contains particularly high levels of Hg (Pokharel and Obrist, 2011). In our study, the soil C and N contents can explain 66% and 57% of the Hg concentration variabilities in soil profiles, respectively (Fig. 7). In addition, we observed the increasing of Hg/C ratio with the decreasing of C/N ratio in the soil profiles (Fig. 8). Two possible causes can explain such Hg accumulation in soil profiles. One is the long-term (decades to hundreds) exposure to atmospheric Hg deposition, thus leading to substantial environmental Hg uptake by the residual SOM (Obrist et al., 2011). The other is that the less loss of Hg than C during the organic matter mineralization leads to a Hg

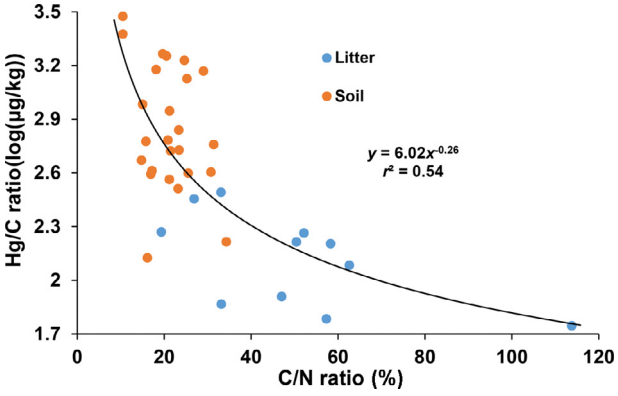


**Fig. 8 – Relationship between Hg/C ratio and C/N ratio for litter and soil samples (soil layers of O, A, B, and C).**

internal accumulation (Obrist et al., 2011) due to the selective Hg adsorption by different organic matter functional groups with various hydrophilic components or molecular weights (Haitzer et al., 2002).

The foliar N and Hg/N ratios in vegetation show insignificant elevation trends ($P > 0.05$), due to the diverse foliage species with large variations in response to the atmospheric N and Hg uptake and the differences of atmospheric N and Hg concentrations along the altitude at Mt. Gongga (Shi et al., 2012). For soil Hg/N ratio, we observed the similar trend as the Hg/C ratio due to the soil N and C both show a higher mineralization rate than Hg during organic soil mineralization (Navrátil et al., 2014). Notably, the higher soil C mineralization rate than N (Melillo et al., 1989) leads to the Hg/C ratio in O horizon 4-fold than in C horizon, but 2-fold for the Hg/N ratio.

## 4. Conclusion

Overall, this study offers an important insight of Hg distribution and the stoichiometric relations among Hg, C, and N along a 3000+ m elevation gradient at Mt. Gongga in the east of the TP. We highlight the vegetation and climate along the

elevation have the controlling impacts on Hg accumulation in forests, but limited influences from (Fig. 4) the soil types induced weathering processes at Mt. Gongga. The surface soil THg in middle elevation forests is significantly higher than that of low/high elevation forests, likely due to the increased litterfall Hg deposition and a lower rate of Hg loss from forest floor in middle elevation forests. In addition, the alpine forest receives less atmospheric Hg depositions than other forest zones because of the high elevation and climatic conditions which significantly constraining the litter biomass production induced Hg depositions. Hence, our results suggest that the montane Hg accumulation does not simply follow the "mountain cold-trapping effect" which refers to an increasing trend of Hg concentration along the elevation. Instead, the enhanced Hg accumulation along the montane elevation depends on the comprehensive effects from the vegetation and climate. We recommend further studies to evaluate the ecological risk to terrestrial biota due to the specific Hg distribution pattern along the montane forests.

## Acknowledgments

This work was funded by the National Natural Science Foundation of China (Nos. 41977272 and 42007307).

REFERENCES

Agnan, Y., Le Dantec, T., Moore, C.W., Edwards, G.C., Obrist, D., 2016. New Constraints on Terrestrial Surface-Atmosphere Fluxes of Gaseous Elemental Mercury Using a Global Database. Environ. Sci. Technol. 50, 507–524.

AMAP/UN Environment, 2019. Technical Background Report to the Global Mercury Assessment. Narayana Press, Gylling, DK-8300 Odder, Denmark 2018 (No. ISBN 978-82-7971-108-7).

Bargagli, R., 2016. Moss and lichen biomonitoring of atmospheric mercury: A review. Sci. Total Environ. 572, 216–231.

Bishop, K.H., Lee, Y.H., Munthe, J., Dambrine, E., 1998. Xylem sap as a pathway for total mercury and methylmercury transport from soils to tree canopy in the boreal forest. Biogeochemistry 40, 101–113.

Blackwell, B.D., Driscoll, C.T., 2015. Deposition of Mercury in Forests along a Montane Elevation Gradient. Environ. Sci. Technol. 49, 5363–5370.

Bravo, A.G., Bouchet, S., Tolu, J., Bjorn, E., Mateos-Rivera, A., Bertilsson, S., 2017. Molecular composition of organic matter controls methylmercury formation in boreal lakes. Nat. Commun. 8, 14255.

Bushey, J.T., Nallana, A.G., Montesdeoca, M.R., Driscoll, C.T., 2008. Mercury dynamics of a northern hardwood canopy. Atmos. Environ. 42, 6905–6914.

Friedli, H.R., Radke, L.F., Payne, N.J., McRae, D.J., Lynham, T.J., Blake, T.W., 2007. Mercury in vegetation and organic soil at an upland boreal forest site in Prince Albert National Park, Saskatchewan, Canada. J. Geophys. Res.-Biogeo. 112.

Fu, X., Feng, X., Wang, S., Rothenberg, S., Shang, L., Li, Z., et al., 2009. Temporal and spatial distributions of total gaseous mercury concentrations in ambient air in a mountainous area in southwestern China: implications for industrial and domestic mercury emissions in remote areas in China. Sci. Total Environ. 407, 2306–2314.

Fu, X., Feng, X., Zhu, W., Rothenberg, S., Yao, H., Zhang, H., 2010. Elevated atmospheric deposition and dynamics of mercury in a remote upland forest of southwestern China. Environ. Pollut. 158, 2324–2333.

Fu, X., Feng, X., Zhu, W., Wang, S., Lu, J., 2008. Total gaseous mercury concentrations in ambient air in the eastern slope of Mt. Gongga, South-Eastern fringe of the Tibetan plateau, China. Atmos. Environ. 42, 970–979.

Fu, X.W., Feng, X., Dong, Z.Q., Yin, R.S., Wang, J.X., Yang, Z.R., Zhang, H., 2010a. Atmospheric gaseous elemental mercury (GEM) concentrations and mercury depositions at a high-altitude mountain peak in south China. Atmos. Chem. Phys. 10, 2425–2437.

Garten Jr., C.T., Hanson, P.J., 2006. Measured forest soil C stocks and estimated turnover times along an elevation gradient. Geoderma 136, 342–352.

Gerson, J.R., Driscoll, C.T., Demers, J.D., Sauer, A.K., Blackwell, B.D., Montesdeoca, M.R., et al., 2017. Deposition of mercury in forests across a montane elevation gradient: Elevational and seasonal patterns in methylmercury inputs and production. J. Geophys. Res.-Biogeo. 122, 1922–1939.

Gong, P., Wang, X.P., Xue, Y.G., Xu, B.Q., Yao, T.D., 2014. Mercury distribution in the foliage and soil profiles of the Tibetan forest: Processes and implications for regional cycling. Environ. Pollut. 188, 94–101.

Grigal, D.F., 2003. Mercury sequestration in forests and peatlands: A review. J. Environ. Qual. 32, 393–405.

Haitzer, M., Aiken, G.R., Ryan, J.N., 2002. Binding of mercury(II) to dissolved organic matter: The role of the mercury-to-DOM concentration ratio. Environ. Sci. Technol. 36, 3564–3570.

Kloeppel, B.D., Gower, S.T., Vogel, J.G., Reich, P.B., 2000. Leaf-level resource use for evergreen and deciduous conifers along a resource availability gradient. Funct. Ecol. 14, 281–292.

Laacouri, A., Nater, E.A., Kolka, R.K., 2013. Distribution and Uptake Dynamics of Mercury in Leaves of Common Deciduous Tree Species in Minnesota, USA. Environ. Sci. Technol. 47, 10462–10470.

Lawson, S.T., Scherbatskoy, T.D., Malcolm, E.G., Keeler, G.J., 2003. Cloud water and throughfall deposition of mercury and trace elements in a high elevation spruce-fir forest at Mt. Mansfield, Vermont. J. Environ. Monitor. 5, 578–583.

Li, Y., Yin, Y., Liu, G., Tachiev, G., Roelant, D., Jiang, G., et al., 2012. Estimation of the Major Source and Sink of Methylmercury in the Florida Everglades. Environ. Sci. Technol. 46, 5885–5893.

Lu, Z., Wang, X., Zhang, Y., Zhang, Y.J., Luo, K., Sha, L., 2016. High mercury accumulation in two subtropical evergreen forests in South China and potential determinants. J. Environ. Manage. 183, 488–496.

Melillo, J.M., Aber, J.D., Linkins, A.E., Ricca, A., Fry, B., Nadelhoffer, K.J., 1989. Carbon and nitrogen dynamics along the decay continuum: Plant litter to soil organic matter. Plant Soil 115, 189–198.

Millhollen, A.G., Gustin, M.S., Obrist, D., 2006. Foliar mercury accumulation and exchange for three tree species. Environ. Sci. Technol. 40, 6001–6006.

Navrátil, T., Shanley, J., Rohovec, J., Hojdová, M., Penížek, V., Buchtová, J., 2014. Distribution and Pools of Mercury in Czech Forest Soils. Water Air Soil Poll. 225.

Obrist, D., Johnson, D.W., Edmonds, R.L., 2012. Effects of vegetation type on mercury concentrations and pools in two adjacent coniferous and deciduous forests. J. Plant Nutr. Soil Sc. 175, 68–77.

Obrist, D., Johnson, D.W., Lindberg, S.E., 2009. Mercury concentrations and pools in four Sierra Nevada forest sites, and relationships to organic carbon and nitrogen. Biogeosciences 6, 765–777.

Obrist, D., Johnson, D.W., Lindberg, S.E., Luo, Y., Hararuk, O., Bracho, R., et al., 2011. Mercury Distribution Across 14 US Forests. Part I: Spatial Patterns of Concentrations in Biomass, Litter, and Soils. Environ. Sci. Technol. 45, 3974–3981.

Pokharel, A.K., Obrist, D., 2011. Fate of mercury in tree litter during decomposition. Biogeosciences 8, 2507–2521.
Pradhan, A., Kumari, S., Dash, S., Biswal, D.P., Dash, A.K., Panigrahi, K.C.S., 2017. Heavy Metal Absorption Efficiency of two Species of Mosses (Physcomitrella patens and Funaria hygrometrica) Studied in Mercury Treated Culture under Laboratory Condition. In: IOP Conference Series: Materials Science and Engineering, p. 225.
Rea, A.W., Lindberg, S.E., Scherbatskoy, T., Keeler, G.J., 2002. Mercury accumulation in foliage over time in two northern mixed-hardwood forests. Water Air Soil Poll. 133, 49–67.
Rewald, B., Ephrath, J.E., Rachmilevitch, S., 2011. A root is a root is a root? Water uptake rates of Citrus root orders. Plant Cell Environ. 34, 33–42.
Shi, W., Wang, G., Han, W., 2012. Altitudinal variation in leaf nitrogen concentration on the eastern slope of Mount Gongga on the Tibetan Plateau, China. PLoS One 7, e44628.
Smith-Downey, N.V., Sunderland, E.M., Jacob, D.J., 2010. Anthropogenic impacts on global storage and emissions of mercury from terrestrial soils: Insights from a new global model. J. Geophys. Res.-Biogeo. 115.
St Louis, V.L., Rudd, J.W.M., Kelly, C.A., Hall, B.D., Rolfhus, K.R., Scott, K.J., et al., 2001. Importance of the forest canopy to fluxes of methyl mercury and total mercury to boreal ecosystems. Environ. Sci. Technol. 35, 3089–3098.
Stankovic, J.D., Sabovljevic, A.D., Sabovljevic, M.S., 2018. Bryophytes and heavy metals: a review. Acta Bot. Croat. 77, 109–118.
Wang, J.J., Guo, Y.Y., Guo, D.L., Yin, S.L., Kong, D.L., Liu, Y.S., et al., 2012. Fine root mercury heterogeneity: metabolism of lower-order roots as an effective route for mercury removal. Environ. Sci. Technol. 46, 769–777.
Wang, X., Luo, J., Yin, R., Yuan, W., Lin, C.J., Sommar, J., et al., 2017. Using Mercury Isotopes To Understand Mercury Accumulation in the Montane Forest Floor of the Eastern Tibetan Plateau. Environ. Sci. Technol. 51, 801–809.
Wang, X., Yuan, W., Feng, X., Wang, D., Luo, J., 2019. Moss facilitating mercury, lead and cadmium enhanced accumulation in organic soils over glacial erratic at Mt. Gongga, China. Environ. Pollut. 254.
Wang, X., Yuan, W., Lin, C.-J., Luo, J., Wang, F., Feng, X., et al., 2020. Underestimated Sink of Atmospheric Mercury in a Deglaciated Forest Chronosequence. Environ. Sci. Technol. 54, 8083–8093.
Wang, X., Yuan, W., Lu, Z., Lin, C.J., Yin, R., Li, F., Feng, X., 2019b. Effects of Precipitation on Mercury Accumulation on Subtropical Montane Forest Floor: Implications on Climate Forcing. J. Geophys. Res.-Biogeo. 124, 959–972.
Xie, J., Zhu, W., Zhou, P., Zhao, G., 2014. Variations in carbon isotope of the main woody plants along the elevational gradient on the Gongga Mountain. J. Nanjing Forest. Univ. (Natur. Sci. Edn.) 38, 33–37.
Yang, Y., Yanai, R.D., Montesdeoca, M., Driscoll, C.T., 2017. Measuring mercury in wood: challenging but important. Int. J. Environ. An. Ch. 97, 456–467.
Zhang, H., Yin, R.S., Feng, X.B., Sommar, J., Anderson, C.W., Sapkota, A., et al., 2013. Atmospheric mercury inputs in montane soils increase with elevation: evidence from mercury isotope signatures. Sci. Rep. 3, 3322.
Zheng, W., Obrist, D., Weis, D., Bergquist, B.A., 2016. Mercury isotope compositions across North American forests. Global Biogeochem. Cy. 30, 1475–1492.
Zhou, J., Feng, X., Liu, H., Zhang, H., Fu, X., Bao, Z., et al., 2013. Examination of total mercury inputs by precipitation and litterfall in a remote upland forest of Southwestern China. Atmos. Environ. 81, 364–372.
Zhou, J., Obrist, D., Dastoor, A., Jiskra, M., Ryjkov, A., 2021. Vegetation uptake of mercury and impacts on global cycling. Nat. Rev. Earth Environ. 2, 269–284.
Zhou, J., Wang, Z., Sun, T., Zhang, H., Zhang, X., 2016. Mercury in terrestrial forested systems with highly elevated mercury deposition in southwestern China: The risk to insects and potential release from wildfires. Environ. Pollut. 212, 188–196.
Zhou, J., Wang, Z.W., Zhang, X.S., Gao, Y., 2017. Mercury concentrations and pools in four adjacent coniferous and deciduous upland forests in Beijing, China. J. Geophys. Res.-Biogeo. 122, 1260–1274.
Zhou, P., Zhu, W., Luo, J., Chen, Y., Yang, Y., Xie, J., 2013b. Aboveground Biomass and Carbon Storage of Typical Forest Types in Gongga Mountain. Xibei Zhiwu Xuebao 33, 162–168.
Zhu, W., Fu, X., Feng, X., Lu, J.Y., 2008. Annual time-series analyses of total gaseous mercury measurement and its impact factors on the Gongga Mountains in the southeastern fringe of the Qinghai-Tibetan Plateau. J. Mt. Sci.-Engl. 5, 17–31.
Zu, K., Luo, A., Shrestha, N., Liu, B., Wang, Z., Zhu, X., 2019. Altitudinal biodiversity patterns of seed plants along Gongga Mountain in the southeastern Qinghai-Tibetan Plateau. Ecol. Evol. 9, 9586–9596.